The SARTOM Project: Tomography and polarimetry for enhanced target detection for foliage penetrating airborne SAR

Nick Walker[1], Ralf Horn[2], Armando Marino[3], Matteo Nannini[2], Iain Woodhouse[3]

1. eOsphere Limited (www.eOsphere.co.uk)
2. German Aerospace Center (DLR)
3. University of Edinburgh

Abstract

The SARTOM project has assessed the value of a range of advanced research techniques to the subject of foliage penetrating radar for the detection and classification of military targets; in particular this has focussed on SAR Tomography and polarimetry. In this paper we present a summary of our results.

Introduction

The SARTOM project has addressed a key area of defence interest, namely the detection and identification of targets hidden in foliage. The project has provided a rich source of data obtained from a series of flight trials that were conducted in September 2006 at a test site near Munich, Germany. This multi-frequency (X-, C- and L-Band) and fully polarimetric data set has been examined with the use of advanced processing techniques designed to extract the maximum amount of information contained in the data: namely SAR Tomography and the analysis of multi-polarimetric scattering characteristics of the foliage and target signatures.

The SARTOM project was able to provide the first demonstration of target detection under foliage using tomography (Figure 1). It also combined tomography with polarimetry to highlight the different scattering mechanisms between the targets and the foliage overhead and in the background (Section 0).

An important aspect of the study has been to address the practicality of the tomographic technique for real applications (Section 0). This has focused on the need to ensure that the technique works without the need for corner reflectors to calibrate the phase in the data and to establish the minimum number of passes required to generate a tomogram.

In supporting work a new polarimetric target detection algorithm has been developed, which, according to our results, outperforms existing algorithms. This is

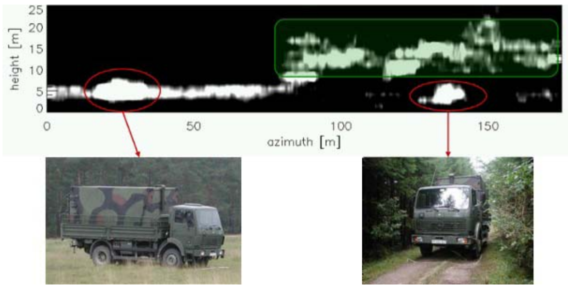

Figure 1. SAR Tomography allows a 3-dimensional picture of a scattering volume to be constructed in contrast to the usual 2-dimensional SAR image. The image shows two military trucks; one situated in a forest and the other in a field. The tomogram is clearly able to identify the truck despite the foliage which can be seen above it.

especially the case for small point targets (such as vehicles) which is why this is of particular interest for defence applications (Section 0). Another important factor is that as well as detecting targets from amongst background clutter the algorithm offers the possibility for target classification.

SAR tomography & polarimetry

SAR tomography [1] is an imaging technique that allows a vertical resolution to be resolved through the construction of a synthetic aperture (tomographic aperture) in the direction perpendicular to the flight path. Hence, separation of multiple phase centres within a resolution cell becomes possible, leading to a 3-dimensional representation of the scene.

By analysing the polarimetry of a backscattered signal it is possible to derive information concerning the main scattering mechanisms related to a target and consequently to characterise it through its signature. In particular, by carrying out a change of basis from the lexicographic (measured by the radar) to the "Pauli basis", it is possible to obtain a three element vector: (monostatic case) that detects for: odd-bounce (Pauli1), even-bounce (Pauli2), and volumetric contributions (Pauli3).

In Figure 2 the results obtained on the SARTOM data using time domain beam-forming (TDB) [2] are shown. This is a coherent processing method that, due to its linearity, allows the combination of all the polarimetric information to be combined in one single colour-coded tomogram.

Incoherent methods like the Capon beam-former [3] have also been investigated.

It can be seen in Figure 2 that the backscattered power of Pauli3 (HV) in correspondence to the target has no significant amplitude when compared with the Pauli1 and Pauli2 components. The truck is represented by the yellow spot located under the canopy that corresponds precisely to the combination of Pauli1 and Pauli3 components. It is interesting to observe that different polarizations detect different parts of the truck (e.g. Pauli1 is more sensitive to the rear part of it, while Pauli2 is more sensitive to the front of it).

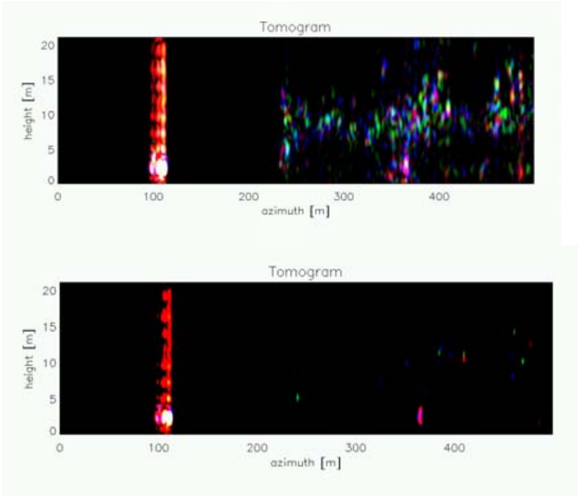

Figure 2. Colour coded polarimetric tomogram in the Pauli basis of the hidden truck by means of the TDB algorithm. R=Pauli2, G=Pauli3, B=Pauli1. In the top image the dynamic range of the image values has been set to provide a reliable representation of the canopy through the Pauli3 contribution. The target outside the forest is represented by the red spot on the left (double bounce) and the target hidden beneath the vegetation is identified by the purple spot. In the bottom image the scaling of the dynamic range has been adjusted so that the hidden target is emphasised (at the azimuth position of ~370m).

Tomography: practicality issues

The tomography results demonstrate that the technique can provide information that is very useful for the detection of targets under foliage; however, the extra price to be paid for this information is considerable, in terms of the number of flight passes to be made over the target and the extra processing required. Two topics have been examined to investigate these practicality issues: (i) Ensuring that it is possible to complete the phase calibration part of the processing without needing to make use of corner reflectors present in the scene, (ii) Examining the effect of reducing the number of passes on the quality of the derived tomogram.

Phase calibration: Figure 3 shows two tomograms where one has been produced using the absolute phase calibration achieved using a corner reflector that was present in the field. The other image shows the tomogram produced using a relative phase calibration made without the corner reflector. It can be seen that the quality of the second tomogram has not suffered appreciably with respect to the former, indicating that this stage of the tomographic processing can be achieved without the need for special equipment to be placed in the field prior to the data acquisition.

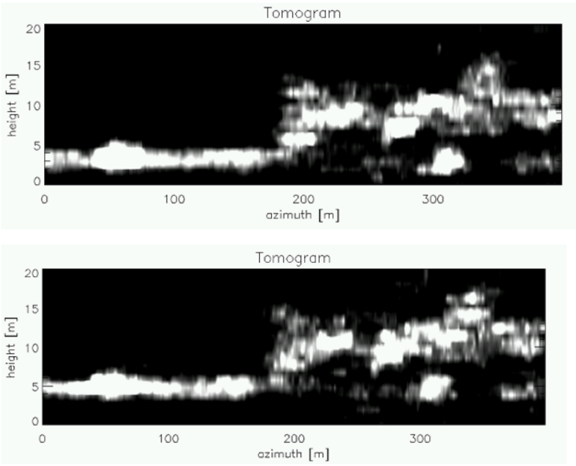

Figure 3. The top image shows the tomogram produced using the absolute phase calibration achieved using a corner reflector. The bottom image shows the tomogram produced using the relative phase calibration made without the corner reflector.

The number of passes: A study has been conducted examining the quality of a tomogram as the number of passes used in its construction is reduced. From the SARTOM trials 22 passes were available for use to construct a tomogram, such as that shown in Figure 1. Clearly it would not be feasible in an operational situation to make this many passes.

The study was conducted using the Capon and the MUSIC algorithmic approaches and is described in more detail in [15]. Figure 4 provides a demonstration of the tomogram that was derived using the MUSIC algorithm using only 6 passes. We hope to pursue this issue further with the aim of establishing the limit on the number of passes, and possibly examining whether different flight pass geometries can assist in reducing the number of passes needed to construct a tomogram that meets our target detection requirements.

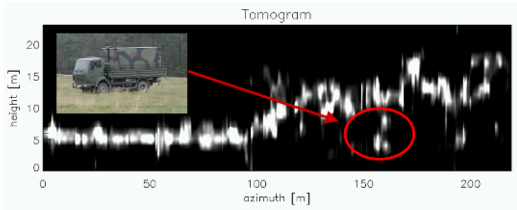

Figure 4. Pseudo-power of the MUSIC algorithm with N=6 tracks. The robustness of the algorithm allows the detection with this reduced constellation.

Enhanced target detection & classification using SAR polarimetry

A target detection algorithm has been developed that exploits a particular aspect of the polarimetric target response which is characterised by a concept known as the polarimetric fork. The detector is not based on a statistical technique, but rather by a physical approach based on sensitivity of the polarimetric complex coherence to changes in polarisation.

Work to-date comparing the new algorithm with previous algorithms has considered PolInSAR techniques (an example of which is that due to Cloude et al [16]), target decomposition theorems (Freeman-Durden [17] and Entropy/alpha/beta [18]) and the polarimetric whitening filter (PWF) due to Novak [19].

The detector is based on the fact that a man-made target can be uniquely characterised by its polarimetric signature, which can be completely encapsulated by the polarisation fork (PF). The PF is composed by a unique set of polarisations related to the physical properties of the target such as its shape and material. In particular this unique set of polarisations is often defined by those specific polarisations that when transmitted have a maximum or minimum return.

It is well known that by transmitting and receiving on only one polarisation (and not the whole set of optimum polarisations) can lead to misclassification of the target since two completely different targets can have exactly the same response for a single polarisation (e.g. different targets can be confused with each other). However, this is not the case for the whole set of optimum polarisations. Fortunately, the optimum polarisations can be reconstructed in post processing starting from the classical fully polarimetric acquisition. By basing the algorithm on the PF the detection is assured to be unique (since the PF is uniquely linked to the single target for a specific viewing geometry).

The algorithm has demonstrated better detection rates to other techniques, including the PWF, which is considered to be optimal in some respects (see Figure 7 and Figure 8). The improved performance is particularly evident for targets hidden under foliage, and in other noisy clutter environments, such as in ploughed fields, where we have been able to achieve a large reduction in the false alarm and missed detection rates.

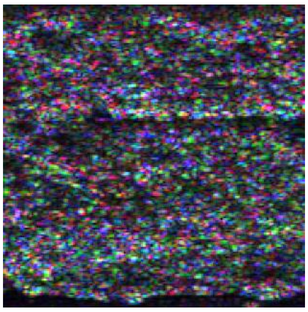

Figure 5. Original SAR image, in Pauli RGB format, geo-located with the two detection images below. In this section of data 3 corner reflectors were hidden under the forest canopy.

Figure 6. One of the 70cm corner reflectors placed under the forest canopy.

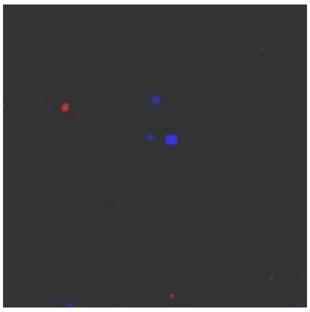

Figure 7. The Marino detector correctly identifies all 3 corner reflectors (in blue) at their correct locations. The "red" detected point represents the double bounce from tree trunks in a small clearing. Similar results were obtained for different military targets hidden under the foliage, and when measured in comparison to other algorithms.

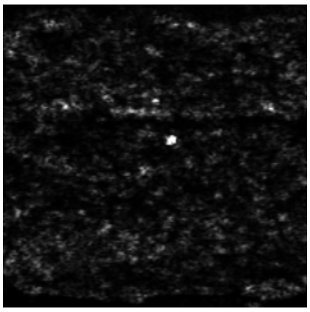

Figure 8. The Polarimetric whitening filter to be compared with the Marino detection algorithm in Figure 7.

Conclusion

The SARTOM project has provided a highly valuable dataset upon which a range of novel techniques have been applied for the purpose of target detection for targets covered by foliage.

Results obtained by means of polarimetric SAR tomography have been presented. The 3D polarimetric analysis completed with the TDB algorithm led to consistent and reliable results that can be exploited to define a signature of the hidden target for target detection purpose.

A study has been conducted seeking to make tomography as practical as possible and attempting to establish the number of passes necessary to produce a useful tomogram.

A new polarimetric target detection algorithm has been developed which only requires the data to be acquired from one pass. Results indicate that this algorithm has a number of features that make it attractive for the detection of targets underneath foliage, or for relatively small targets in a high clutter background. This is due to the fact that the algorithm's formalism allows for the characterisation of the target to be established, making target classification possible, and because the algorithm makes use of the target's polarimetric scattering properties rather than the scattering strength of the target.

Acknowledgements

The work reported in this paper was funded by the Electro-magnetic Remote Sensing (EMRS) Defence Technology Centre, established by the UK Ministry of Defence and run by a consortium of SELEX Galileo, Thales UK and Roke Manor Research.

References

[1] Reigber and A. Moreira, First Demonstration of Airborne SAR Tomography using multibaseline L-Band Data, IEEE Trans. on Geosc. and Remote Sensing Vol. 38, no.5, pp.2142-2152, 2000

[2] M. Nannini and R. Scheiber, A Time Domain Beamforming Algorithm for SAR Tomography, Proc. EUSAR conf., Dresden, 16-18 May, 2006A.G. Thomas, M.C. Berg, "Medium PRF set selection: an approach through combinatorics.", *IEE Proc.-Radar, Sonar Navig.*,, Vol. 141, No. 6, December 1994, pp.307- 311

[3] F. Lombardini and A. Reigber, Adaptative spectral estimation for multibaseline SAR Tomography with airborne L-band data, in Proc. IGARSS, Toulouse, France, 2003

[4] M. A. Karam, A. K. Fung, R. H. Lang, and N. S. Chuahuan, "A microwave scattering model for layered vegetation," IEEE Transaction on Geoscience and Remote Sensing, vol. 30, pp. 799-808, 1992.

[5] S. S. Saatchi and K. C. Mcdonald, "Coherent effects in microwave backscattering models for forest canopies," IEEE Transaction on Geoscience and Remote Sensing, vol. 35, 1997.

[6] J. G. Fleishman, S. Ayasli, E. M. Adams, and D. R. Gosselin, "Foliage penetration experiment Part I: Foliage attenuation and backscatter analysis of SAR imagery," IEEE Transaction on Aerospace and Electronic Systems, vol. 32, 1996.

[7] R. N. Treuhaft, S. N. Madesen, M. Moghaddam, and J. J. Van Zyl, "Vegetation characteristics and underlying topography for interferometric radar," Radio Science, vol. 31, 1996.

[8] S. R. Cloude and K. P. Papathanassiou, "Polarimetric SAR interferometry," IEEE Transaction on

Geoscience and Remote sensing, vol. 36, 1998.

[9] J. K. Niklas, Plant allometry: the scaling of form and process. Chicago: The University of Chicago Press, 1994.

[10] Y. Oh, K. Sarabandi, and F. T. Ulaby, "An empirical model and an inversion technique for radar scattering from bare soil surface," IEEE Transaction on Geoscience and Remote Sensing, vol. 30, pp. 370-381, 1992.

[11] J. A. Richards, G. Q. Sun, and D. S. Simonett, "L-band radar backscatter of forest stands," IEEE Transaction on Geoscience and Remote Sensing, vol. 25, pp. 487-498, 1987.

[12] I. H. Woodhouse, Introduction to Microwave Remote Sensing. London: Taylor and Francis, 2006.

[13] R. Horn, M. Nannini, and M. Keller, "SARTOM airborne campaign 2006 data acquisition report," 2006.

[14] S. R. Cloude and E. Pottier, "A review of target decomposition theorems in radar polarimetry," IEEE Transaction on Geoscience and Remote Sensing, vol. 34, 1996.

[15] Nannini M., Scheiber R., Moreira A. “Estimation of the minimum number of tracks for SAR tomography”, IEEE Transaction on Geoscience and Remote Sensing, February 2009.

[16] S R Cloude, D G Corr and M LWilliams, “Target detection beneath foliage using polarimetric synthetic aperture radar interferometry.” Waves Random Media 14 (2004) S393–S414.

[17] Freeman and S. L. Durden, "A Three-Component Scattering Model for Polarimetric SAR Data," IEEE Transaction on Geosciences and Remote Sensing, vol. 36, pp. 963-973, 1998.

[18] J. Lee, M. R. Grunes, T. L. Ainsworth, L. J. Du, D. L. Schuler, and S. R. Cloude, "Unsupervised Classification Using Polarimetric Decomposition and the Complex Wishart Classifier," IEEE Transaction on Geosciences and Remote Sensing, vol. 37, pp. 2249-2258, 1999.

[19] L. M. Novak, M. C. Burl, and M. W. Irving, "Optimal Polarimetric Processing for Enhanced Target Detection," IEEE Trans. Aerospace and Electronic Systems, vol. 20, pp. 234-244, 1993.